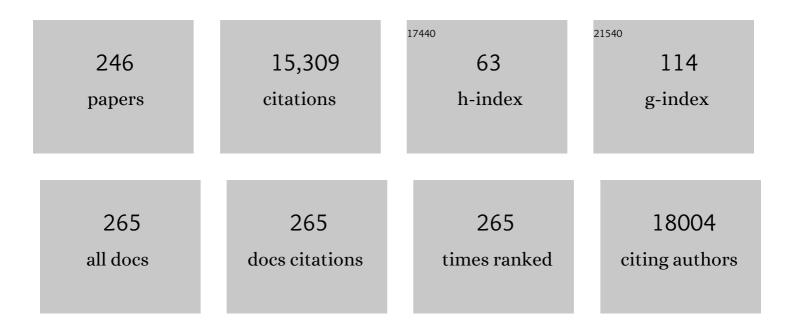
Weiping Cai

List of Publications by Year in descending order

Source: https://exaly.com/author-pdf/4557387/publications.pdf Version: 2024-02-01



#	Article	IF	CITATIONS
1	Au Polyhedron Array with Tunable Crystal Facets by PVPâ€Assisted Thermodynamic Control and Its Sharp Shape As Well As Highâ€Energy Exposed Planes Coâ€Boosted SERS Activity. Small, 2022, 18, e2105045.	10.0	16
2	Microporousâ€Ceriaâ€Wrapped Gold Nanoparticles for Conductometric and SERS Dual Monitoring of Hazardous Gases at Room Temperature. Advanced Materials Interfaces, 2022, 9, .	3.7	5
3	Onion-structured transition metal dichalcogenide nanoparticles by laser fabrication in liquids and atmospheres. Chinese Physics B, 2022, 31, 076106.	1.4	1
4	Fabrication of Pt–Ag–Au heterogeneous truncated hollow sub-microspheres for chemically self-propelled colloidal motors. Nano Futures, 2022, 6, 025003.	2.2	1
5	Surface Roughening of Pt-Polystyrene Spherical Janus Micromotors for Enhanced Motion Speed. Micromachines, 2022, 13, 555.	2.9	4
6	Abnormally Weak Surface-Enhanced Raman Scattering Activity of Tip-Rich Au Nanostars: The Role of Interfacial Defects. Journal of Physical Chemistry Letters, 2022, 13, 2428-2433.	4.6	2
7	High-Density-Nanotips-Composed 3D Hierarchical Au/CuS Hybrids for Sensitive, Signal-Reproducible, and Substrate-Recyclable SERS Detection. Nanomaterials, 2022, 12, 2359.	4.1	1
8	One-Pot Synthesis of Ultrasmooth, Precisely Shaped Gold Nanospheres via Surface Self-Polishing Etching and Regrowth. Chemistry of Materials, 2021, 33, 2593-2603.	6.7	29
9	Quantitative Surface-Enhanced Raman Spectroscopy for Field Detections Based on Structurally Homogeneous Silver-Coated Silicon Nanocone Arrays. ACS Omega, 2021, 6, 18928-18938.	3.5	22
10	Hydrogel Film@Au Nanoparticle Arrays Based on Selfâ€Assembly Coâ€Assisted by Electrostatic Attraction and Hydrogel‧hrinkage for SERS Detection with Active Gaps. Advanced Materials Interfaces, 2021, 8, 2101055.	3.7	13
11	Defective-tin-oxide wrapped gold nanoparticles with strong sunlight harvesting and efficient charge separation for photocatalysis. Chemical Engineering Journal, 2021, 420, 129981.	12.7	8
12	Ultrasensitive surface-enhanced Raman spectroscopy detection of gaseous sulfur-mustard simulant based on thin oxide-coated gold nanocone arrays. Journal of Hazardous Materials, 2021, 420, 126668.	12.4	17
13	A sensitive colorimetric chiral recognition for thiol-containing amino acids based on NIR plasmonic MoO _{3â^'<i>x</i>} nanoparticles. Journal of Materials Chemistry C, 2021, 9, 11091-11097.	5.5	3
14	A universal route with fine kinetic control to a family of penta-twinned gold nanocrystals. Chemical Science, 2021, 12, 12631-12639.	7.4	15
15	Convective Self-Assembly of 2D Nonclose-Packed Binary Au Nanoparticle Arrays with Tunable Optical Properties. Chemistry of Materials, 2021, 33, 310-319.	6.7	38
16	Optimal Excitation Wavelength for Surface-Enhanced Raman Spectroscopy: The Role of Chemical Interface Damping. Journal of Physical Chemistry Letters, 2021, 12, 11014-11021.	4.6	6
17	Engineering of flexible granular Au nanocap ordered array and its surface enhanced Raman spectroscopy effect. Nanotechnology, 2020, 31, 035303.	2.6	6
18	Rapid and ultrasensitive surface-enhanced Raman spectroscopy detection of mercury ions with gold film supported organometallic nanobelts. Nanotechnology, 2020, 31, 155501.	2.6	8

#	Article	IF	CITATIONS
19	Mars–van-Krevelen mechanism-based blackening of nano-sized white semiconducting oxides for synergetic solar photo-thermocatalytic degradation of dye pollutants. Nanoscale, 2020, 12, 4030-4039.	5.6	12
20	Monodispersed Snowman-Like Ag-MoS ₂ Janus Nanoparticles as Chemically Self-Propelled Nanomotors. ACS Applied Nano Materials, 2020, 3, 624-632.	5.0	16
21	Highly Selective and Sensitive Detection of Hydrogen Sulfide by the Diffraction Peak of Periodic Au Nanoparticle Array with Silver Coating. ACS Applied Materials & Interfaces, 2020, 12, 40702-40710.	8.0	19
22	Ultra-fast synthesis of water soluble MoO3â ^{~,} x quantum dots with controlled oxygen vacancies and their near infrared fluorescence sensing to detect H2O2. Nanoscale Horizons, 2020, 5, 1538-1543.	8.0	16
23	Ordered gold-coated glass nano-sting array with large density tips as highly SERS-active chips for detection of trace organophosphorous toxicant. Nanotechnology, 2020, 31, 415301.	2.6	5
24	Raman reporter-assisted Au nanorod arrays SERS nanoprobe for ultrasensitive detection of mercuric ion (Hg2+) with superior anti-interference performances. Journal of Hazardous Materials, 2020, 398, 122890.	12.4	51
25	Conductometric Response-Triggered Surface-Enhanced Raman Spectroscopy for Accurate Gas Recognition and Monitoring Based on Oxide-wrapped Metal Nanoparticles. ACS Sensors, 2020, 5, 1641-1649.	7.8	9
26	Ultrathin layer solid transformation-enabled-surface enhanced Raman spectroscopy for trace harmful small gaseous molecule detection. Nanoscale Horizons, 2020, 5, 739-746.	8.0	11
27	Two-dimensional flower-shaped Au@Ag nanoparticle arrays as effective SERS substrates with high sensitivity and reproducibility for detection of thiram. Journal of Materials Chemistry C, 2020, 8, 3838-3845.	5.5	29
28	Ultrathin Hexagonal PbO Nanosheets Induced by Laser Ablation in Water for Chemically Trapping Surface-Enhanced Raman Spectroscopy Chips and Detection of Trace Gaseous H2S. ACS Applied Materials & Interfaces, 2020, 12, 23330-23339.	8.0	14
29	Crâ€Dopant Induced Breaking of Scaling Relations in CoFe Layered Double Hydroxides for Improvement of Oxygen Evolution Reaction. Small, 2019, 15, e1902373.	10.0	111
30	Airâ€Liquid Interfacial Selfâ€Assembly of Twoâ€Dimensional Periodic Nanostructured Arrays. ChemNanoMat, 2019, 5, 1338-1360.	2.8	34
31	Ultrathin and Isotropic Metal Sulfide Wrapping on Plasmonic Metal Nanoparticles for Surface Enhanced Ram Scattering-Based Detection of Trace Heavy-Metal Ions. ACS Applied Materials & Interfaces, 2019, 11, 28145-28153.	8.0	19
32	Monodispersed Zerovalent Iron Nanoparticles Decorated Carbon Submicrospheres for Enhanced Removal of DDT from Aqueous Solutions. ChemistrySelect, 2019, 4, 12134-12142.	1.5	6
33	Porous zeolite imidazole framework-wrapped urchin-like Au-Ag nanocrystals for SERS detection of trace hexachlorocyclohexane pesticides via efficient enrichment. Journal of Hazardous Materials, 2019, 368, 429-435.	12.4	72
34	4-Mercaptophenylboronic acid modified Au nanosheets-built hollow sub-microcubes for active capture and ultrasensitive SERS-based detection of hexachlorocyclohexane pesticides. Sensors and Actuators B: Chemical, 2019, 293, 63-70.	7.8	18
35	Status and demand of research to bring laser generation of nanoparticles in liquids to maturity. Applied Surface Science, 2019, 488, 445-454.	6.1	61
36	Fabrication of Ag-nanosheets-built micro/nanostructured arrays via <i>in situ</i> conversion on Cu ₂ O-coated Si nanocone platform and their highly structurally-enhanced SERS effect. Nanotechnology, 2019, 30, 345302.	2.6	12

#	Article	IF	CITATIONS
37	Highly sensitive detection of nitrite by using gold nanoparticle-decorated α-Fe ₂ O ₃ nanorod arrays as self-supporting photo-electrodes. Inorganic Chemistry Frontiers, 2019, 6, 1432-1441.	6.0	18
38	Flexible vanadium-doped Ni ₂ P nanosheet arrays grown on carbon cloth for an efficient hydrogen evolution reaction. Nanoscale, 2019, 11, 4198-4203.	5.6	122
39	Bilayer Au nanoparticle-decorated WO3 porous thin films: On-chip fabrication and enhanced NO2 gas sensing performances with high selectivity. Sensors and Actuators B: Chemical, 2019, 280, 192-200.	7.8	61
40	N-doping nanoporous carbon microspheres derived from MOFs for highly efficient removal of formaldehyde. Nanotechnology, 2019, 30, 105702.	2.6	14
41	Laser Synthesis of Colloids: Fundamentals and Applications. World Scientific Series in Nanoscience and Nanotechnology, 2019, , 183-211.	0.1	0
42	Ultrasensitive and Stable Au Dimerâ€Based Colorimetric Sensors Using the Dynamically Tunable Gapâ€Đependent Plasmonic Coupling Optical Properties. Advanced Functional Materials, 2018, 28, 1707392.	14.9	48
43	Periodic Porous Alloyed Au–Ag Nanosphere Arrays and Their Highly Sensitive SERS Performance with Good Reproducibility and High Density of Hotspots. ACS Applied Materials & Interfaces, 2018, 10, 9792-9801.	8.0	138
44	Bionic PDMS film with hybrid superhydrophilic/superhydrophobic arrays for water harvest. Surface Innovations, 2018, 6, 141-149.	2.3	15
45	Decoration of Au Nanoparticles on MoS ₂ Nanospheres: From Janus to Core/Shell Structure. Journal of Physical Chemistry C, 2018, 122, 8628-8636.	3.1	18
46	3â€Acrylamidophenylboronic Acidâ€Modified Hydrogel Film Attached to a Gold Nanosphere Array to Detect Hydrofluoric Acid with Good Selectivity and Recyclability. ChemNanoMat, 2018, 4, 165-169.	2.8	6
47	Micro/nanostructured porous ZnO as a new DGT binding phase for selective measurement of Cu(II) in water. Colloids and Surfaces A: Physicochemical and Engineering Aspects, 2018, 537, 109-115.	4.7	12
48	Strong SERS Performances of Ultrathin α o(OH) ₂ Nanosheets to the Toxic Organophosphorus Molecules and Hydrogen Bondâ€Induced Charge Transfer Mechanism. Advanced Materials Interfaces, 2018, 5, 1700709.	3.7	13
49	Tailoring Surface Opening of Hollow Nanocubes and Their Application as Nanocargo Carriers. ACS Central Science, 2018, 4, 1742-1750.	11.3	13
50	Large-Scale Synthesis of Co/CoO _{<i>x</i>} Encapsulated in Nitrogen-, Oxygen-, and Sulfur-Tridoped Three-Dimensional Porous Carbon as Efficient Electrocatalysts for Hydrogen Evolution Reaction. ACS Applied Energy Materials, 2018, 1, 6250-6259.	5.1	15
51	Ni _{0.33} Co _{0.67} MoS ₄ nanosheets as a bifunctional electrolytic water catalyst for overall water splitting. Journal of Materials Chemistry A, 2018, 6, 19555-19562.	10.3	50
52	Controllable corrosion-assisted fabrication of Au–Ag alloyed hollow nanocrystals for highly efficient and environmentally-stable SERS substrates. Nanotechnology, 2018, 29, 455604.	2.6	5
53	Large Area α-Cu ₂ S Particle-Stacked Nanorod Arrays by Laser Ablation in Liquid and Their Strong Structurally Enhanced and Stable Visible Photoelectric Performances. ACS Applied Materials & Interfaces, 2018, 10, 19027-19036.	8.0	20
54	Ball Milling-Induced Plate-like Sub-microstructured Iron for Enhancing Degradation of DDT in a Real Soil Environment. ACS Omega, 2018, 3, 6955-6961.	3.5	5

#	Article	IF	CITATIONS
55	Laser-irradiation induced synthesis of spongy AuAgPt alloy nanospheres with high-index facets, rich grain boundaries and subtle lattice distortion for enhanced electrocatalytic activity. Journal of Materials Chemistry A, 2018, 6, 13735-13742.	10.3	32
56	Cu-Doped CoP Nanorod Arrays: Efficient and Durable Hydrogen Evolution Reaction Electrocatalysts at All pH Values. ACS Applied Energy Materials, 2018, 1, 3835-3842.	5.1	58
57	Strong Electronic Interaction in Dualâ€Cationâ€Incorporated NiSe ₂ Nanosheets with Lattice Distortion for Highly Efficient Overall Water Splitting. Advanced Materials, 2018, 30, e1802121.	21.0	361
58	Kinetically-Controlled Growth of Chestnut-Like Au Nanocrystals with High-Density Tips and Their High SERS Performances on Organochlorine Pesticides. Nanomaterials, 2018, 8, 560.	4.1	7
59	MnMoO ₄ nanosheet array: an efficient electrocatalyst for hydrogen evolution reaction with enhanced activity over a wide pH range. Nanotechnology, 2018, 29, 335403.	2.6	17
60	Bifunctional Hybrid Ni/Ni ₂ P Nanoparticles Encapsulated by Graphitic Carbon Supported with N, S Modified 3D Carbon Framework for Highly Efficient Overall Water Splitting. Advanced Materials Interfaces, 2018, 5, 1800473.	3.7	40
61	Interaction properties between different modes of localized and propagating surface plasmons in a dimer nanoparticle array. Optical Engineering, 2018, 57, 1.	1.0	6
62	Oneâ€Step and Surfactantâ€Free Fabrication of Goldâ€Nanoparticleâ€Decorated Bismuth Oxychloride Nanosheets Based on Laser Ablation in Solution and Their Enhanced Visibleâ€Light Plasmonic Photocatalysis. ChemPhysChem, 2017, 18, 1146-1154.	2.1	9
63	Capillary Gradientâ€Induced Selfâ€Assembly of Periodic Au Spherical Nanoparticle Arrays on an Ultralarge Scale via a Bisolvent System at Air/Water Interface. Advanced Materials Interfaces, 2017, 4, 1600976.	3.7	48
64	Structure and thickness-dependent gas sensing responses to NO 2 under UV irradiation for the multilayered ZnO micro/nanostructured porous thin films. Journal of Colloid and Interface Science, 2017, 503, 150-158.	9.4	45
65	Nanoscaled Amorphous TiO ₂ Hollow Spheres: TiCl ₄ Liquid Droplet-Based Hydrolysis Fabrication and Strong Hollow Structure-Enhanced Surface-Enhanced Raman Scattering Effects. Langmuir, 2017, 33, 5430-5438.	3.5	16
66	Hierarchical micro/nanostructured C doped Co/Co ₃ O ₄ hollow spheres derived from PS@Co(OH) ₂ for the oxygen evolution reaction. Journal of Materials Chemistry A, 2017, 5, 11163-11170.	10.3	61
67	Surface enhanced Raman scattering properties of dynamically tunable nanogaps between Au nanoparticles self-assembled on hydrogel microspheres controlled by pH. Journal of Colloid and Interface Science, 2017, 505, 467-475.	9.4	23
68	"Close network―effect of a ZnO micro/nanoporous array allows high UV-irradiated NO ₂ sensing performance. RSC Advances, 2017, 7, 21054-21060.	3.6	12
69	Functionalized periodic Au@MOFs nanoparticle arrays as biosensors for dual-channel detection through the complementary effect of SPR and diffraction peaks. Nano Research, 2017, 10, 2257-2270.	10.4	44
70	S,N-Containing Co-MOF derived Co ₉ S ₈ @S,N-doped carbon materials as efficient oxygen electrocatalysts and supercapacitor electrode materials. Inorganic Chemistry Frontiers, 2017, 4, 491-498.	6.0	108
71	Ultrathin Oxide Layer-Wrapped Noble Metal Nanoparticles via Colloidal Electrostatic Self-Assembly for Efficient and Reusable Surface Enhanced Raman Scattering Substrates. Langmuir, 2017, 33, 12934-12942.	3.5	10
72	Controlled synthesis of sponge-like porous Au–Ag alloy nanocubes for surface-enhanced Raman scattering properties. Journal of Materials Chemistry C, 2017, 5, 11039-11045.	5.5	45

#	Article	IF	CITATIONS
73	Temperature regulation growth of Au nanocrystals: from concave trisoctahedron to dendritic structures and their ultrasensitive SERS-based detection of lindane. Journal of Materials Chemistry C, 2017, 5, 10399-10405.	5.5	23
74	Onion-Structured Spherical MoS ₂ Nanoparticles Induced by Laser Ablation in Water and Liquid Droplets' Radial Solidification/Oriented Growth Mechanism. Journal of Physical Chemistry C, 2017, 121, 23233-23239.	3.1	15
75	Mn doped porous cobalt nitride nanowires with high activity for water oxidation under both alkaline and neutral conditions. Chemical Communications, 2017, 53, 13237-13240.	4.1	53
76	SERS-based ultrasensitive detection of organophosphorus nerve agents via substrate's surface modification. Journal of Hazardous Materials, 2017, 324, 194-202.	12.4	52
77	Ultrathin tin oxide layer-wrapped gold nanoparticles induced by laser ablation in solutions and their enhanced performances. Journal of Colloid and Interface Science, 2017, 489, 92-99.	9.4	15
78	Design and fabrication of micro-nano fusion gas sensor based on two-beam micro-hotplatform. Microsystem Technologies, 2017, 23, 2699-2705.	2.0	1
79	Highly efficient removal of hexavalent chromium in aqueous solutions <i>via</i> chemical reduction of plate-like micro/nanostructured zero valent iron. RSC Advances, 2017, 7, 55905-55911.	3.6	37
80	Morphological and Structural Control of Organic Monolayer Colloidal Crystal Based on Plasma Etching and Its Application in Fabrication of Ordered Gold Nanostructured Arrays. Crystals, 2016, 6, 126.	2.2	11
81	A nanoparticulate liquid binding phase based DGT device for aquatic arsenic measurement. Talanta, 2016, 160, 225-232.	5.5	15
82	Metal-organic framework derived nitrogen-doped porous carbon@graphene sandwich-like structured composites as bifunctional electrocatalysts for oxygen reduction and evolution reactions. Carbon, 2016, 106, 74-83.	10.3	206
83	Ultrafine nickel–cobalt alloy nanoparticles incorporated into three-dimensional porous graphitic carbon as an electrode material for supercapacitors. Journal of Materials Chemistry A, 2016, 4, 17080-17086.	10.3	53
84	Fabrication of αâ€Fe ₂ O ₃ porous array film and its crystallization effect on its H ₂ S sensing properties. ChemistrySelect, 2016, 1, 2377-2382.	1.5	7
85	Polyaniline nanofibers and their self-assembly into a film to be used as ammonia sensor. RSC Advances, 2016, 6, 103185-103191.	3.6	13
86	Auâ€NPâ€Decorated Crystalline FeOCl Nanosheet: Facile Synthesis by Laser Ablation in Liquid and its Exclusive Gas Sensing Response to HCl at Room Temperature. Advanced Materials Interfaces, 2016, 3, 1500801.	3.7	37
87	Room temperature H2S gas sensing properties of In2O3 micro/nanostructured porous thin film and hydrolyzation-induced enhanced sensing mechanism. Sensors and Actuators B: Chemical, 2016, 228, 74-84.	7.8	90
88	Complete Au@ZnO core–shell nanoparticles with enhanced plasmonic absorption enabling significantly improved photocatalysis. Nanoscale, 2016, 8, 10774-10782.	5.6	94
89	Enhanced degradation performances of plate-like micro/nanostructured zero valent iron to DDT. Journal of Hazardous Materials, 2016, 307, 145-153.	12.4	30
90	Green and Tunable Decoration of Graphene with Spherical Nanoparticles Based on Laser Ablation in Water: A Case of Ag Nanoparticle/Graphene Oxide Sheet Composites. Langmuir, 2016, 32, 1667-1673.	3.5	21

#	Article	IF	CITATIONS
91	Nanosheets-built flowerlike micro/nanostructured Bi 2 O 2.33 and its highly efficient iodine removal performances. Chemical Engineering Journal, 2016, 289, 219-230.	12.7	77
92	Response and stability improvement by fusing optimized micro-hotplatform and double layer bowl-like nano arrays. Sensors and Actuators B: Chemical, 2016, 231, 450-457.	7.8	9
93	A functional hydrogel film attached with a 2D Au nanosphere array and its ultrahigh optical diffraction intensity as a visualized sensor. Journal of Materials Chemistry C, 2016, 4, 2117-2122.	5.5	45
94	Copper nanoparticle@graphene composite arrays and their enhanced catalytic performance. Acta Materialia, 2016, 105, 59-67.	7.9	62
95	Detection of dimethyl methylphosphonate by thin water film confined surface-enhanced Raman scattering method. Journal of Hazardous Materials, 2016, 303, 94-100.	12.4	15
96	Water bath synthesis and enhanced photocatalytic performances of urchin-like micro/nanostructured α-FeOOH. Journal of Materials Research, 2015, 30, 1629-1638.	2.6	21
97	Monodispersed Particles: Monodispersed Nb ₂ O ₅ Microspheres: Facile Synthesis, Air/Water Interfacial Selfâ€Assembly, Nb ₂ O ₅ â€Based Composite Films, and Their Selective NO ₂ Sensing (Adv. Mater. Interfaces 11/2015). Advanced Materials Interfaces. 2015, 2, .	3.7	2
98	Monodispersed Nb ₂ O ₅ Microspheres: Facile Synthesis, Air/Water Interfacial Selfâ€Assembly, Nb ₂ O ₅ â€Based Composite Films, and Their Selective NO ₂ Sensing. Advanced Materials Interfaces, 2015, 2, 1500167.	3.7	62
99	Spherical Nanoparticle Arrays with Tunable Nanogaps and Their Hydrophobicity Enhanced Rapid SERS Detection by Localized Concentration of Droplet Evaporation. Advanced Materials Interfaces, 2015, 2, 1500031.	3.7	78
100	Electrophoretic fabrication of silver nanostructure/zinc oxide nanorod heterogeneous arrays with excellent SERS performance. Journal of Materials Chemistry C, 2015, 3, 1724-1731.	5.5	14
101	Micro/Nano Gas Sensors: A New Strategy Towards In-Situ Wafer-Level Fabrication of High-Performance Gas Sensing Chips. Scientific Reports, 2015, 5, 10507.	3.3	53
102	Quantum dot-assembled mesoporous CuO nanospheres based on laser ablation in water. RSC Advances, 2015, 5, 19479-19483.	3.6	12
103	Aligned gold nanobowl arrays: their fabrication, anisotropic optical response and optical grating applications. Journal of Materials Chemistry C, 2015, 3, 51-57.	5.5	18
104	Rapid Synthesis of Monodisperse Au Nanospheres through a Laser Irradiation -Induced Shape Conversion, Self-Assembly and Their Electromagnetic Coupling SERS Enhancement. Scientific Reports, 2015, 5, 7686.	3.3	114
105	Micro/nanostructured porous Fe–Ni binary oxide and its enhanced arsenic adsorption performances. Journal of Colloid and Interface Science, 2015, 458, 94-102.	9.4	45
106	Janus gas: reversible redox transition of Sarin enables its selective detection by an ethanol modified nanoporous SnO ₂ chemiresistor. Chemical Communications, 2015, 51, 8193-8196.	4.1	31
107	In situ synthesis of porous array films on a filament induced micro-gap electrode pair and their use as resistance-type gas sensors with enhanced performances. Nanoscale, 2015, 7, 14264-14271.	5.6	24
108	Fabrication of silver nanoplate hierarchical turreted ordered array and its application in trace analyses. Chemical Communications, 2015, 51, 6609-6612.	4.1	36

#	Article	IF	CITATIONS
109	Optical sensor based on hydrogel films with 2D colloidal arrays attached on both the surfaces: anti-curling performance and enhanced optical diffraction intensity. Journal of Materials Chemistry C, 2015, 3, 3659-3665.	5.5	40
110	Self-curled coral-like Î ³ -Al 2 O 3 nanoplates for use as an adsorbent. Journal of Colloid and Interface Science, 2015, 453, 244-251.	9.4	38
111	Fabrication of gold and silver hierarchically micro/nanostructured arrays by localized electrocrystallization for application as SERS substrates. Journal of Materials Chemistry C, 2015, 3, 5709-5714.	5.5	19
112	Black Gold: Plasmonic Colloidosomes with Broadband Absorption Selfâ€Assembled from Monodispersed Gold Nanospheres by Using a Reverse Emulsion System. Angewandte Chemie - International Edition, 2015, 54, 9596-9600.	13.8	189
113	Micro/nano-scaled carbon spheres based on hydrothermal carbonization of agarose. Colloids and Surfaces A: Physicochemical and Engineering Aspects, 2015, 484, 386-393.	4.7	53
114	Physical Deposition Improved SERS Stability of Morphology Controlled Periodic Micro/Nanostructured Arrays Based on Colloidal Templates. Small, 2015, 11, 844-853.	10.0	138
115	Sodiumâ€Doped ZnO Nanowires Grown by Highâ€pressure <scp>PLD</scp> and their Acceptorâ€Related Optical Properties. Journal of the American Ceramic Society, 2014, 97, 2177-2184.	3.8	26
116	Hierarchical ZnO films with microplate/nanohole structures induced by precursor concentration and colloidal templates, their superhydrophobicity, and enhanced photocatalytic performance. Journal of Materials Research, 2014, 29, 115-122.	2.6	10
117	A controlled Ag–Au bimetallic nanoshelled microsphere array and its improved surface-enhanced Raman scattering effect. RSC Advances, 2014, 4, 8758.	3.6	25
118	Wet Etching-Assisted Colloidal Lithography: A General Strategy toward Nanodisk and Nanohole Arrays on Arbitrary Substrates. ACS Applied Materials & Interfaces, 2014, 6, 9207-9213.	8.0	32
119	Tungsten oxide nanostructures based on laser ablation in water and a hydrothermal route. CrystEngComm, 2014, 16, 2491-2498.	2.6	28
120	Gold Binaryâ€ 5 tructured Arrays Based on Monolayer Colloidal Crystals and Their Optical Properties. Small, 2014, 10, 2374-2381.	10.0	25
121	Controllable Synthesis of Well-aligned ZnO Nanorod Arrays on Varying Substrates via Rapid Electrodeposition. Journal of Materials Science and Technology, 2014, 30, 1118-1123.	10.7	15
122	Optical Materials: Gold Binary-Structured Arrays Based on Monolayer Colloidal Crystals and Their Optical Properties (Small 12/2014). Small, 2014, 10, 2373-2373.	10.0	0
123	CuO–ZnO Micro/Nanoporous Arrayâ€Filmâ€Based Chemosensors: New Sensing Properties to H ₂ S. Chemistry - A European Journal, 2014, 20, 6040-6046.	3.3	64
124	Fabrication of Gold Nanoparticles by Laser Ablation in Liquid and Their Application for Simultaneous Electrochemical Detection of Cd ²⁺ , Pb ²⁺ , Cu ²⁺ , Hg ²⁺ . ACS Applied Materials & Interfaces, 2014, 6, 65-71.	8.0	155
125	Au nanoparticle-built mesoporous films based on co-electrophoresis deposition and selective etching. Electrochemistry Communications, 2014, 46, 71-74.	4.7	6
126	An Invisible Template Method toward Gold Regular Arrays of Nanoflowers by Electrodeposition. Langmuir, 2013, 29, 3512-3517.	3.5	35

#	Article	IF	CITATIONS
127	Synthesis of nano-cubic ZnSn(OH)3 based on stannate reaction with liquid laser ablation-induced ZnO below room temperature. CrystEngComm, 2013, 15, 6159.	2.6	14
128	ZnO hollow microspheres with exposed porous nanosheets surface: Structurally enhanced adsorption towards heavy metal ions. Colloids and Surfaces A: Physicochemical and Engineering Aspects, 2013, 422, 199-205.	4.7	86
129	Crackâ€Free Periodic Porous Thin Films Assisted by Plasma Irradiation at Low Temperature and Their Enhanced Gasâ€Sensing Performance. Chemistry - A European Journal, 2013, 19, 13387-13395.	3.3	31
130	One-step fabrication of high performance micro/nanostructured Fe3S4–C magnetic adsorbent with easy recovery and regeneration properties. CrystEngComm, 2013, 15, 2956.	2.6	40
131	Rutile TiO2 films with 100% exposed pyramid-shaped (111) surface: photoelectron transport properties under UV and visible light irradiation. Journal of Materials Chemistry A, 2013, 1, 2646.	10.3	39
132	Fast-Response, Sensitivitive and Low-Powered Chemosensors by Fusing Nanostructured Porous Thin Film and IDEs-Microheater Chip. Scientific Reports, 2013, 3, 1669.	3.3	121
133	Fabrication of porous Ag hollow sphere arrays based on coated template-plasma bombardment. Nanotechnology, 2013, 24, 465302.	2.6	8
134	Physical processes-aided periodic micro/nanostructured arrays by colloidal template technique: fabrication and applications. Chemical Society Reviews, 2013, 42, 3614.	38.1	171
135	Trace detection of cyanide based on SERS effect of Ag nanoplate-built hollow microsphere arrays. Journal of Hazardous Materials, 2013, 248-249, 435-441.	12.4	57
136	Layer-controlled synthesis of WO3 ordered nanoporous films for optimum electrochromic application. Nanoscale, 2013, 5, 2460.	5.6	46
137	Fabrication of Self-Standing Silver Nanoplate Arrays by Seed-Decorated Electrochemical Route and Their Structure-Induced Properties. Journal of Nanomaterials, 2013, 2013, 1-7.	2.7	13
138	Ultra high performance gas sensor based on IC compatible fusion of micromachined hotplatform and nanostructured porous film. , 2013, , .		0
139	Micro/nanostructured α-Fe2O3 spheres: synthesis, characterization, and structurally enhanced visible-light photocatalytic activity. Journal of Materials Chemistry, 2012, 22, 9704.	6.7	103
140	Three-dimensional hierarchically structured PAN@γ–AlOOH fiber films based on a fiber templated hydrothermal route and their recyclable strong Cr(vi)-removal performance. RSC Advances, 2012, 2, 1769.	3.6	35
141	Fabrication and Characterization of Beaded SiC Quantum Rings with Anomalous Red Spectral Shift. Advanced Materials, 2012, 24, 5598-5603.	21.0	65
142	Tunable Surface Plasmon Resonance and Strong SERS Performances of Au Opening-Nanoshell Ordered Arrays. ACS Applied Materials & Interfaces, 2012, 4, 1-5.	8.0	71
143	Core–shell TaxO@Ta2O5 structured nanoparticles: laser ablation synthesis in liquid, structure and photocatalytic property. CrystEngComm, 2012, 14, 3236.	2.6	27
144	Ag Nanoparticle Decorated Nanoporous ZnO Microrods and Their Enhanced Photocatalytic Activities. ACS Applied Materials & Interfaces, 2012, 4, 6030-6037.	8.0	292

#	Article	IF	CITATIONS
145	Photoacoustic Spectroscopy and Its Applications in Characterization of Nanomaterials. , 2012, , 621-649.		0
146	Standing porous ZnO nanoplate-built hollow microspheres and kinetically controlled dissolution/crystal growth mechanism. Journal of Materials Research, 2012, 27, 951-958.	2.6	14
147	Phase Diagram, Design of Monolayer Binary Colloidal Crystals, and Their Fabrication Based on Ethanol-Assisted Self-Assembly at the Air/Water Interface. ACS Nano, 2012, 6, 6706-6716.	14.6	186
148	Standing Ag nanoplate-built hollow microsphere arrays: Controllable structural parameters and strong SERS performances. Journal of Materials Chemistry, 2012, 22, 3177.	6.7	51
149	Defect-Mediated Formation of Ag Cluster-Doped TiO ₂ Nanoparticles for Efficient Photodegradation of Pentachlorophenol. Langmuir, 2012, 28, 3938-3944.	3.5	152
150	Fluorescent Probes: Well-Defined Nanoclusters as Fluorescent Nanosensors: A Case Study on Au25(SG)18 (Small 13/2012). Small, 2012, 8, 2027-2027.	10.0	6
151	Nanomaterials via Laser Ablation/Irradiation in Liquid: A Review. Advanced Functional Materials, 2012, 22, 1333-1353.	14.9	775
152	Leaf-like Tungsten Oxide Nanoplatelets Induced by Laser Ablation in Liquid and Subsequent Aging. Crystal Growth and Design, 2012, 12, 2646-2652.	3.0	62
153	Organization of Mn3O4nanoparticles into γ-MnOOHnanowiresvia hydrothermal treatment of the colloids induced by laser ablation in water. CrystEngComm, 2011, 13, 1063-1066.	2.6	31
154	Gold quasi rod-shaped nanoparticle-built hierarchically micro/nanostructured pore array via clean electrodeposition on a colloidal monolayer and its structurally enhanced SERS performance. Journal of Materials Chemistry, 2011, 21, 8816.	6.7	30
155	Hydrothermal treatment of colloids induced via liquid-phase laser ablation: a new approach for hierarchical titanate nanostructures with enhanced photodegradation performance. CrystEngComm, 2011, 13, 4676.	2.6	12
156	Fabrication of cuprous oxide nanoparticles by laser ablation in PVP aqueous solution. RSC Advances, 2011, 1, 847.	3.6	66
157	Reply to "Comment on â€~From Nanoparticles to Nanoplates: Preferential Oriented Connection of Ag Colloids during Electrophoretic Deposition'― Journal of Physical Chemistry C, 2011, 115, 4982-4983.	3.1	2
158	Reshaping Formation and Luminescence Evolution of ZnO Quantum Dots by Laser-Induced Fragmentation in Liquid. Journal of Physical Chemistry C, 2011, 115, 5038-5043.	3.1	70
159	Polyacrylonitrile/ferrous chloride composite porous nanofibers and their strong Cr-removal performance. Journal of Materials Chemistry, 2011, 21, 991-997.	6.7	108
160	Protein assisted hydrothermal synthesis of ultrafine magnetite nanoparticle built-porous oriented fibers and their structurally enhanced adsorption to toxic chemicals in solution. Journal of Materials Chemistry, 2011, 21, 11188.	6.7	28
161	Luminescent hollow carbon shells and fullerene-like carbon spheres produced by laser ablation with toluene. Journal of Materials Chemistry, 2011, 21, 4432.	6.7	87
162	A General Strategy for Fabricating Unique Carbide Nanostructures with Excitation Wavelength-Dependent Light Emissions. Journal of Physical Chemistry C, 2011, 115, 7279-7284.	3.1	30

#	Article	IF	CITATIONS
163	Origin of Blue Emission from Silicon Nanoparticles: Direct Transition and Interface Recombination. Journal of Physical Chemistry C, 2011, 115, 21056-21062.	3.1	92
164	Influences of Target and Liquid Media on Morphologies and Optical Properties of <scp>ZnO</scp> Nanoparticles Prepared by Laser Ablation in Solution. Journal of the American Ceramic Society, 2011, 94, 4305-4309.	3.8	18
165	Complex nanostructures synthesized from nanoparticle colloids under an external electric field. Nanoscale, 2011, 3, 3933.	5.6	11
166	Blue Luminescence of ZnO Nanoparticles Based on Nonâ€Equilibrium Processes: Defect Origins and Emission Controls. Advanced Functional Materials, 2010, 20, 561-572.	14.9	1,540
167	Surface Nanometerâ€5cale Patterning in Realizing Largeâ€5cale Ordered Arrays of Metallic Nanoshells with Wellâ€Defined Structures and Controllable Properties. Advanced Functional Materials, 2010, 20, 2527-2533.	14.9	124
168	Micro/Nanostructured Ordered Porous Films and Their Structurally Induced Control of the Gas Sensing Performances. Advanced Functional Materials, 2010, 20, 3765-3773.	14.9	83
169	Orientable pore-size-distribution of ZnO nanostructures and their superior photocatalytic activity. CrystEngComm, 2010, 12, 2821.	2.6	31
170	General Synthesis of 2D Ordered Hollow Sphere Arrays Based on Nonshadow Deposition Dominated Colloidal Lithography. Langmuir, 2010, 26, 6295-6302.	3.5	46
171	Surface Decoration of ZnO Nanorod Arrays by Electrophoresis in the Au Colloidal Solution Prepared by Laser Ablation in Water. Langmuir, 2010, 26, 8925-8932.	3.5	83
172	Metal ion-doped SnO2 ordered porous films and their strong gas sensing selectivity. Applied Physics Letters, 2010, 96, .	3.3	41
173	Resistance Reduction Induced by Small Electric Current in CoCu Porous Films. Journal of Physical Chemistry C, 2010, 114, 2300-2304.	3.1	2
174	Vertically cross-linking silver nanoplate arrays with controllable density based on seed-assisted electrochemical growth and their structurally enhanced SERS activity. Journal of Materials Chemistry, 2010, 20, 767-772.	6.7	58
175	Mass production of micro/nanostructured porous ZnO plates and their strong structurally enhanced and selective adsorption performance for environmental remediation. Journal of Materials Chemistry, 2010, 20, 8582.	6.7	216
176	Au nanochain-built 3D netlike porous films based on laser ablation in water and electrophoretic deposition. Chemical Communications, 2010, 46, 7223.	4.1	51
177	Ultra-fine β-SiC quantum dots fabricated by laser ablation in reactive liquid at room temperature and their violet emission. Journal of Materials Chemistry, 2009, 19, 7119.	6.7	79
178	Hetero-apertured Micro/Nanostructured Ordered Porous Array: Layer-by-Layered Construction and Structure-Induced Sensing Parameter Controllability. ACS Nano, 2009, 3, 2697-2705.	14.6	65
179	Controllable Fabrication and Tunable Magnetism of Nickel Nanostructured Ordered Porous Arrays. Journal of Physical Chemistry C, 2009, 113, 3973-3977.	3.1	19
180	In situ self-assembly synthesis and photocatalytic performance of hierarchical Bi0.5Na0.5TiO3 micro/nanostructures. Journal of Materials Chemistry, 2009, 19, 2253.	6.7	49

#	Article	IF	CITATIONS
181	Dramatic excitation dependence of strong and stable blue luminescence of ZnO hollow nanoparticles. Applied Physics Letters, 2009, 95, 191904.	3.3	38
182	Design and Electrochemical Fabrication of Gold Binary Ordered Micro/Nanostructured Porous Arrays via Step-by-Step Colloidal Lithography. Langmuir, 2009, 25, 2558-2562.	3.5	21
183	Optical Study of Redox Behavior of Silicon Nanoparticles Induced by Laser Ablation in Liquid. Journal of Physical Chemistry C, 2009, 113, 6480-6484.	3.1	39
184	From Nanoparticles to Nanoplates: Preferential Oriented Connection of Ag Colloids during Electrophoretic Deposition. Journal of Physical Chemistry C, 2009, 113, 7692-7696.	3.1	44
185	General and Simple Route to Micro/Nanostructured Hollow-Sphere Arrays Based on Electrophoresis of Colloids Induced by Laser Ablation in Liquid. Langmuir, 2009, 25, 8287-8291.	3.5	39
186	Size and Structure Control of Si Nanoparticles by Laser Ablation in Different Liquid Media and Further Centrifugation Classification. Journal of Physical Chemistry C, 2009, 113, 19091-19095.	3.1	112
187	Template-induced synthesis of hierarchical SiO ₂ <i>@</i> γ-AlOOH spheres and their application in Cr(VI) removal. Nanotechnology, 2009, 20, 155604.	2.6	52
188	Layer-by-layer strategy for the general synthesis of 2D ordered micro/nanostructured porous arrays: structural, morphological and compositional controllability. Journal of Materials Chemistry, 2009, 19, 7301.	6.7	28
189	Room temperature synthesized rutile TiO ₂ nanoparticles induced by laser ablation in liquid and their photocatalytic activity. Nanotechnology, 2009, 20, 285707.	2.6	103
190	ZnO Hierarchical Micro/Nanoarchitectures: Solvothermal Synthesis and Structurally Enhanced Photocatalytic Performance. Advanced Functional Materials, 2008, 18, 1047-1056.	14.9	580
191	Magnetic step regions in α-Fe2O3 nanostructured ring arrays. Physica E: Low-Dimensional Systems and Nanostructures, 2008, 40, 680-683.	2.7	7
192	Ordered Micro/Nanostructured Arrays Based on the Monolayer Colloidal Crystals. Chemistry of Materials, 2008, 20, 615-624.	6.7	240
193	Fabrication and Size-Dependent Optical Properties of FeO Nanoparticles Induced by Laser Ablation in a Liquid Medium. Journal of Physical Chemistry C, 2008, 112, 3261-3266.	3.1	105
194	Wettability and Superhydrophobicity of 2-D Ordered Nano-structured Arrays Based on Colloidal Monolayers. Journal of Adhesion Science and Technology, 2008, 22, 1949-1965.	2.6	10
195	Controllable Pt/ZnO Porous Nanocages with Improved Photocatalytic Activity. Journal of Physical Chemistry C, 2008, 112, 19620-19624.	3.1	157
196	Ordered n-type ZnO nanorod arrays. Applied Physics Letters, 2008, 92, 132112.	3.3	61
197	From ZnO Nanorods to Nanoplates:  Chemical Bath Deposition Growth and Surface-Related Emissions. Journal of Physical Chemistry C, 2008, 112, 680-685.	3.1	225
198	Trapeziform Ag Nanosheet Arrays Induced by Electrochemical Deposition on Au-Coated Substrate. Crystal Growth and Design, 2008, 8, 2748-2752.	3.0	37

#	Article	IF	CITATIONS
199	Aging-Induced Strong Anomalous Hall Effect at Room Temperature for Cu(Co) Nanoparticle Film. Journal of Physical Chemistry C, 2008, 112, 1837-1841.	3.1	5
200	Unconventional Method for Morphology-Controlled Carbonaceous Nanoarrays Based on Electron Irradiation of a Polystyrene Colloidal Monolayer. ACS Nano, 2008, 2, 1108-1112.	14.6	81
201	Polycrystalline Si nanoparticles and their strong aging enhancement of blue photoluminescence. Journal of Applied Physics, 2008, 104, 023516.	2.5	49
202	Aging-Induced Self-Assembly of Zn/ZnO Treelike Nanostructures from Nanoparticles and Enhanced Visible Emission. Crystal Growth and Design, 2007, 7, 1092-1097.	3.0	56
203	Silver Hierarchical Bowl-Like Array:  Synthesis, Superhydrophobicity, and Optical Properties. Langmuir, 2007, 23, 9802-9807.	3.5	170
204	Microstructure Control of Zn/ZnO Core/Shell Nanoparticles and Their Temperature-Dependent Blue Emissions. Journal of Physical Chemistry B, 2007, 111, 14311-14317.	2.6	143
205	High-Yield Synthesis of Single-Crystalline Gold Nano-octahedra. Angewandte Chemie - International Edition, 2007, 46, 3264-3268.	13.8	209
206	Controllable superhydrophobic and lipophobic properties of ordered pore indium oxide array films. Journal of Colloid and Interface Science, 2007, 314, 615-620.	9.4	33
207	Hierarchical Structured Ni Nanoring and Hollow Sphere Arrays by Morphology Inheritance Based on Ordered Through-Pore Template and Electrodeposition. Journal of Physical Chemistry B, 2006, 110, 15729-15733.	2.6	75
208	Transferable Ordered Ni Hollow Sphere Arrays Induced by Electrodeposition on Colloidal Monolayer. Journal of Physical Chemistry B, 2006, 110, 7184-7188.	2.6	64
209	Two-dimensional hierarchical porous silica film and its tunable superhydrophobicity. Nanotechnology, 2006, 17, 238-243.	2.6	144
210	Morphology-controlled 2D ordered arrays by heating-induced deformation of 2D colloidal monolayer. Journal of Materials Chemistry, 2006, 16, 609-612.	6.7	43
211	Electrochemically induced flowerlike gold nanoarchitectures and their strong surface-enhanced Raman scattering effect. Applied Physics Letters, 2006, 89, 211905.	3.3	112
212	Hierarchical surface rough ordered Au particle arrays and their surface enhanced Raman scattering. Applied Physics Letters, 2006, 89, 181918.	3.3	89
213	Ultrasonically Induced Au Nanoprisms and Their Size Manipulation Based on Aging. Journal of Physical Chemistry B, 2006, 110, 1546-1552.	2.6	58
214	Growth of ZnO Nanoneedle Arrays with Strong Ultraviolet Emissions by an Electrochemical Deposition Method. Crystal Growth and Design, 2006, 6, 1091-1095.	3.0	68
215	Fabrication of the periodic nanopillar arrays by heat-induced deformation of 2D polymer colloidal monolayer. Polymer, 2005, 46, 12033-12036.	3.8	28
216	2D nanoparticle arrays by partial dissolution of ordered pore films. Materials Letters, 2005, 59, 276-279.	2.6	17

#	Article	IF	CITATIONS
217	Superhydrophobicity of 2D ZnO ordered pore arrays formed by solution-dipping template method. Journal of Colloid and Interface Science, 2005, 287, 634-639.	9.4	172
218	Two-dimensional ordered polymer hollow sphere and convex structure arrays based on monolayer pore films. Journal of Materials Research, 2005, 20, 338-343.	2.6	21
219	Optical studies of polyvinylpyrrolidone reduction effect on free and complex metal ions. Journal of Materials Research, 2005, 20, 320-324.	2.6	68
220	Composition/Structural Evolution and Optical Properties of ZnO/Zn Nanoparticles by Laser Ablation in Liquid Media. Journal of Physical Chemistry B, 2005, 109, 18260-18266.	2.6	353
221	Ultraviolet-light-emitting ZnO nanosheets prepared by a chemical bath deposition method. Nanotechnology, 2005, 16, 1734-1738.	2.6	124
222	Tree-like Ag nanostructures based on monolithic mesoporous silica. Journal of Materials Research, 2004, 19, 1328-1332.	2.6	5
223	An ambience-induced optical absorption peak for Au/SiO2 mesoporous assembly. Chemical Physics Letters, 2004, 385, 15-19.	2.6	11
224	Fabrication of large-scale zinc oxide ordered pore arrays with controllable morphology. Chemical Communications, 2004, , 1604.	4.1	55
225	Ultrasonic solvent induced morphological change of Au colloids. Materials Letters, 2004, 58, 196-199.	2.6	17
226	Reduction effect of pore wall and formation of Au nanowires inside monolithic mesoporous silica. Chemical Physics Letters, 2003, 382, 318-324.	2.6	30
227	Controllable optical properties of Au/SiO2 nanocomposite induced by ultrasonic irradiation and thermal annealing. Applied Physics Letters, 2003, 83, 36-38.	3.3	29
228	Optical study of the ultrasonic formation process of noble metal nanoparticles dispersed inside the pores of monolithic mesoporous silica. Journal Physics D: Applied Physics, 2003, 36, 1382-1387.	2.8	10
229	Optical Absorption of Copper Nanoparticles Dispersed within Pores of Monolithic Mesoporous Silica. Journal of Materials Research, 2002, 17, 1125-1128.	2.6	25
230	Optical absorption of Ag oligomers dispersed within pores of mesoporous silica. Chemical Physics Letters, 2002, 357, 249-254.	2.6	27
231	Sonochemical Processes and Formation of Gold Nanoparticles within Pores of Mesoporous Silica. Journal of Colloid and Interface Science, 2001, 238, 291-295.	9.4	166
232	Title is missing!. Journal of Nanoparticle Research, 2001, 3, 441-451.	1.9	45
233	Preparation and optical absorption of gold nanoparticles within pores of mesoporous silica. Materials Research Bulletin, 2000, 35, 1689-1695.	5.2	40
234	Composition modulation of optical absorption in AgxAu1â´'x alloy nanocrystals in situ formed within pores of mesoporous silica. Journal of Applied Physics, 2000, 87, 1572-1574.	2.5	104

#	Article	IF	CITATIONS
235	Synthesis and luminescence of the nanosized Ce-doped silica particles dispersed within the pores of mesoporous silica host. Journal of Materials Research, 1999, 14, 1922-1927.	2.6	5
236	Luminescence of aggregated and dispersed nanosized cerium doped silica particles. Journal of Materials Science Letters, 1999, 18, 1849-1851.	0.5	2
237	Photoluminescence of indium–oxide nanoparticles dispersed within pores of mesoporous silica. Applied Physics Letters, 1999, 75, 495-497.	3.3	186
238	Semiconductor optical features of silver / silica mesoporous composite. Science Bulletin, 1998, 43, 614-615.	1.7	1
239	Ambience-induced alternating change of optical absorption for the porous silica host loaded with silver nanometer particles. Applied Physics A: Materials Science and Processing, 1998, 66, 419-422.	2.3	9
240	Optical measurements of oxidation behavior of silver nanometer particle within pores of silica host. Journal of Applied Physics, 1998, 83, 1705-1710.	2.5	81
241	Annealing of mesoporous silica loaded with silver nanoparticles within its pores from isothermal sorption. Journal of Materials Research, 1998, 13, 2888-2895.	2.6	43
242	Semiconducting optical properties of silver/silica mesoporous composite. Applied Physics Letters, 1998, 73, 2709-2711.	3.3	68
243	Optical absorption of ZnS nanocrystals inside pores of silica. Applied Physics Letters, 1997, 71, 3697-3699.	3.3	37
244	Reversible transition between transparency and opacity for the porous silica host dispersed with silver nanometer particles within its pores. Applied Physics Letters, 1996, 69, 2980-2982.	3.3	37
245	Ultrathin Oxide Wrapping of Plasmonic Nanoparticles via Colloidal Electrostatic Self-Assembly and their Enhanced Performances. , 0, , .		1

246 SERS-Based Sensitive Detection of Organophosphorus Nerve Agents. , 0, , .

0